Chapter 6: Turbulent Transport and its Modeling

Part 2: Lagrangian Analysis of Turbulent Transport

Gradient transport law requires mixing length $(l) \ll$ region over which mean velocity can be assumed linear. For turbulent transport, l determined by eddy size/action $\gg$ molecular mean free path as per molecular viscosity which is relevant viscous shear stress tensor.

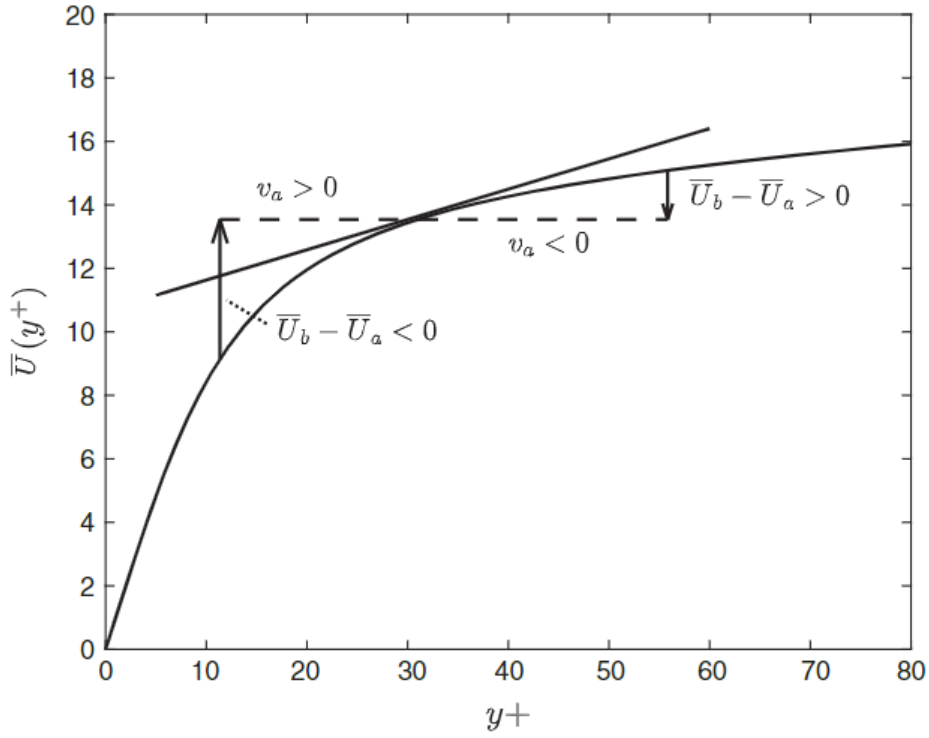

Figure 6.2 A local linear approximation to the mean velocity field $\overline{U}$ at a point a in a channel flow is inappropriate for fluid particles traveling significant distances during the mixing time. Fluid particles traveling toward the wall located at $y^+ = 0$ have $v_a < 0$, $\overline{U}_b - \overline{U}_a > 0$, and vice versa for particles traveling away from the wall.

Figure shows linear approximation mean velocity profile is only valid for very small distances.

However, concept that turbulent mixing in which fluid particles carry momentum from initial to final points over a mixing time to cause net momentum transport may have some validity.

To analyze the validity of

$$\sigma_{12}^{T} = -\rho\overline{uv} = \mu_T \frac{\partial \overline{U}}{\partial y}$$

using $\underline{U} = \overline{U} + \underline{u}$ nomenclature, the turbulent motions that cause u and v to be correlated are explored using DNS data for channel flow.

Figure 6.3 Ensemble of paths, each with a different initial position **b**, arriving at **a**.

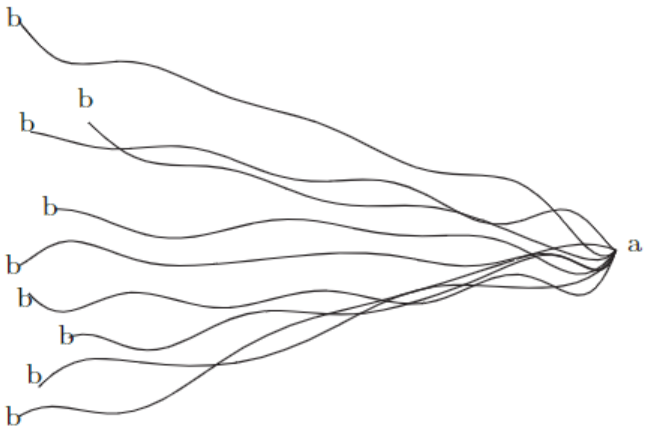

Consider set of particles arriving at $\underline{a}$ at time t, which originated at $\underline{b}$ following various paths $\underline{X}(s)$ such that $\underline{X}(t) = \underline{a}$ and $\underline{X}(t-\tau) = \underline{b}$ where $\underline{X}(s)$ and $\underline{b}$ are a random ensemble of realizations. $\tau > 0$ = motion at earlier times than t. Note that s = time such that $s < t$ = motion prior arrival at $\underline{a}$ and $s > t$ = future time.

$$\frac{d\underline{X}(s)}{ds} = \underline{U}\big(\underline{X}(s), s\big) = \langle \underline{U} \rangle \big(\underline{X}(s), s\big) + \underline{u}\big(\underline{X}(s), s\big) \quad (1)$$

Lagrangian | Eulerian | Reynolds decomposition using ensemble average where both terms are random since $\underline{X}(s)$

At time t:

$$\underline{U_a} = \langle \underline{U_a} \rangle + \underline{u_a} \quad (2)$$

At time $t - \tau$:

$$\underline{U_b} = \langle \underline{U_b} \rangle + \underline{u_b} \quad (3)$$

Integration of Eq. (1) between $t-\tau$ and t gives:

$$\int_{t-\tau}^{t} d\underline{X}(s) = \int_{t-\tau}^{t} \underline{U}\big(\underline{X}(s), s\big) ds$$

$$\underline{a} - \underline{b} = \underline{L} = \int_{t-\tau}^{t} \underline{U}\big(\underline{X}(s), s\big) ds$$

s = time

Where $\underline{L}$ represents the change in (time average) particle position from $\underline{b}$ to $\underline{a}$ in time τ.

Eq. (2) minus Eq. (3) gives:

$$u_a = u_b + \underbrace{(\langle U_b \rangle - \langle U_a \rangle)}_{\boxed{1}} + \underbrace{(U_a - U_b)}_{\boxed{2}} \quad (4)$$

Scalar version of Eqs. (2) and (3) for x-component

Where $\langle U_b \rangle$ represents the ensemble average = sum of all b velocities divided by number of b particles; and similarly, for $\langle U_a \rangle$.

Eq. (4) expresses u_a in terms of value at earlier time u_b plus factors that led to its change.

1) Change in local mean (ensemble average) velocity field between b and a.
2) Change in instantaneous velocity due to acceleration or deceleration caused by pressure or viscous forces = difference in instantaneous values of velocities.

Thus, even for $U_b = U_a$, i.e., non-accelerating flow $u_a \neq u_b$ due to changes in local mean velocity.

Multiply Eq. (4) by v_a and time average yields

$$\overline{u_a v_a} = \underbrace{\overline{u_b v_a}}_{\boxed{1}} + \underbrace{\overline{v_a(\langle U_b \rangle - \langle U_a \rangle)}}_{\boxed{2}} + \underbrace{\overline{v_a(U_a - U_b)}}_{\boxed{3}} \quad (5)$$

Note for statistically stationary flow (at the same point) time average = ensemble average, i.e., $\langle U_a \rangle = \overline{U}_a$.

In Eq. (5) $\overline{u_a v_a}$ represents the Reynolds stress σ_{12}^T, such that $u_a v_a$ is time averaged between $t - \tau$ and t.

For small τ, $\overline{u_b v_a}$ converges to $\overline{u_a v_a}$, whereas for large τ, $\overline{u_b v_a}$ goes to zero, which gives an upper limit to the mixing time.

Term 2 is referred to as displacement transport term $= \Phi_{\mathrm{D}} = \overline{v_a(\langle U_b \rangle - \langle U_a \rangle)}$ and represents momentum transport due to eddy mixing over time interval for which $\overline{u_a v_a}$ is correlated. If locally, the mean velocity is linear this term will yield gradient diffusion/eddy-viscosity model, as will be shown later using its Taylor series representation.

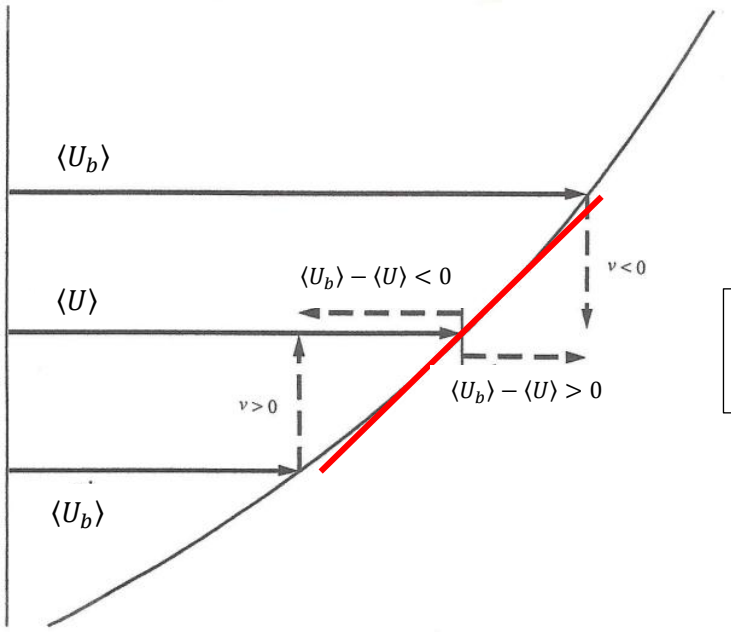

In this figure $\langle U \rangle = \langle U_a \rangle$

Fig. 6.7 Source of displacement transport correlation.

Note $\Phi_{\mathrm{D}} < 0$ since for $v_a < 0$, $\langle U_b \rangle - \langle U_a \rangle > 0$ and for $v_a > 0$, $\langle U_b \rangle - \langle U_a \rangle < 0$.

Term 3 is referred as Φ_{A} and is absent in the molecular model (and gradient model) since molecules are assumed to retain their momentum over the mixing time.

Channel Flow DNS

$$Eq.(5) = \overline{f}(\tau) = \frac{1}{\tau}\int_{t-\tau}^{t} v_a(Eq.4)dt$$

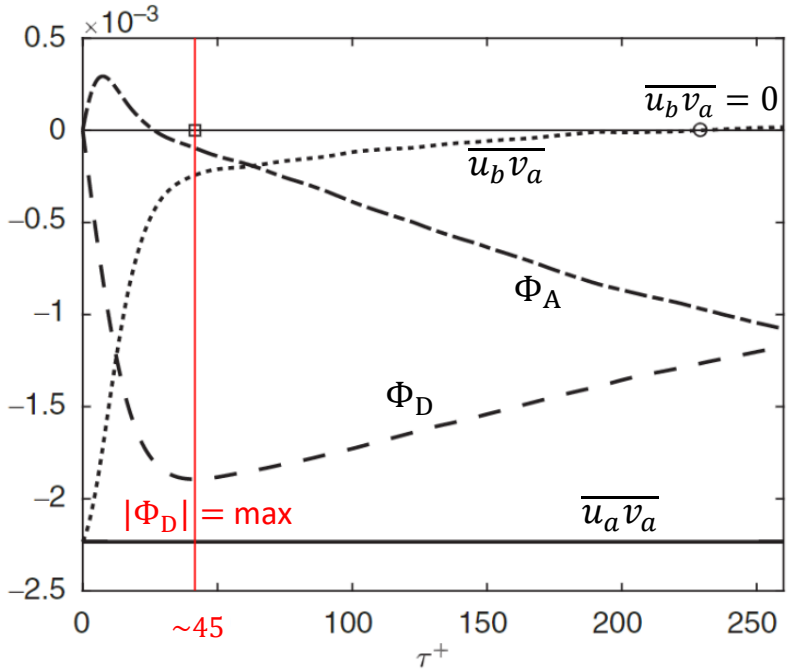

$y^+ = \frac{yU_\tau}{\nu}$ = 54.8

$U_\tau = \left[\nu \frac{d\overline{U}}{dy}(0)\right]^{1/2} = \sqrt{\frac{\tau_w}{\rho}}$

U_τ = friction velocity

$\tau^+ = \frac{\tau U_\tau}{y}$

For all τ^+ values, the sum of $\overline{u_b v_a}$, Φ_A and Φ_D must equal $\overline{u_a v_a}$, but magnitude of each term varies with τ^+.

$\overline{u_b v_a}$ goes to zero for large $\tau^+ = \frac{\tau U_\tau}{y}$, whereas for $\tau^+ = 0$, $\overline{u_a v_a} = \overline{u_b v_a}$.

Φ_A trend for short-term ($\tau^+ < 100$) strongly depends on y^+ (not shown), although $\Phi_A(\tau^+ = 0) = 0$. For large τ^+, independent of y^+, and its value tends to $\overline{u_a v_a}$.

At $\tau^+ = 0$, $a \equiv b$, i.e., $\overline{v_a\langle U_b\rangle} = \overline{v_a\langle U_a\rangle} = 0$

$$\Phi_A = \overline{v_a(U_a - U_b)} = \overline{v_a(\langle U_a\rangle + u_a)} - \overline{v_a(\langle U_b\rangle + u_b)}$$

$$= \overline{v_a\langle U_a\rangle} + \overline{v_a u_a} - \overline{v_a\langle U_b\rangle} - \overline{v_a u_b}$$

$\overline{f\langle g\rangle} = 0$

$= 0$ for all τ^+

Goes to 0 as $\tau^+ \to \infty$

Goes to 0 as $\tau^+ \to \infty$

No correlation between a and b as their distance increases

Φ_D decreases towards a minimum value close in value to $\overline{u_a v_a}$ before rising back towards zero. For large τ^+, $\Phi_D \to 0$

$$\Phi_D = \overline{v_a(\langle U_b\rangle - \langle U_a\rangle)} = \overline{v_a\langle U_b\rangle} - \overline{v_a\langle U_a\rangle} = \overline{v_a\langle U_b\rangle}$$

Goes to 0 as $\tau^+ \to \infty$

$= 0$ for all τ^+

Φ_D minimum same order of magnitude as $\overline{u_a v_a}$ at time τ_D = mixing time as reflects most closely idea of gradient hypothesis.

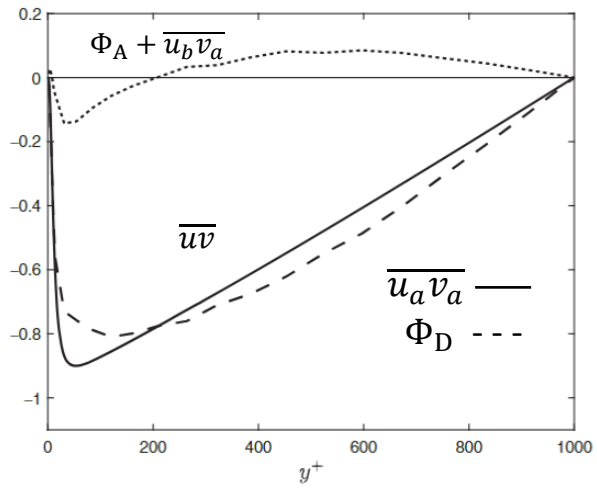

Lower half of channel
$0 < y^+ < 1000$
Time averaging from t-τ_D to t. Showing that gradient model works for this flow and conditions.

$$Eq.(5) = \overline{f}(\tau_d) = \frac{1}{\tau_d}\int_{t-\tau_d}^{t} v_a(Eq.4)dt$$

Figure 6.5 Evaluation of Eq. (6.24) at τ_D computed across the channel. —, $\overline{u_a v_a}$; – –, $\overline{(\overline{U}_b - \overline{U}_a)v_a}$; · · · , $\overline{(U_a - U_b)v_a} + \overline{u_b v_a}$.

$\overline{uv} < 0$ = transport u towards wall

Shows $\overline{uv} = \overline{vu} \approx \Phi_D = \overline{v_a\langle U_b\rangle}$ and Term 1 + Term 3 only small effect at time τ_D. The form of $\Phi_D = \overline{v_a\langle U_b\rangle}$ suggests the nature of the u and v correlations, which produce $\overline{uv}$.

Conclusion:

For averaging $0 \le \tau^+ \le \tau_D$: $\Phi_D \approx \overline{u_a v_a}$ and $\Phi_A + \overline{u_b v_a}$ relatively small

Whereas for averaging $0 \le \tau^+ \le \infty$: $\Phi_A = \overline{u_a v_a}$ and $\Phi_D = 0$.

Since τ represents the time/spatial difference between $\underline{a}$ and $\underline{b}$, and for $\tau = \tau_D$ $\Phi_D \approx \overline{uv}$, τ_D therefore defines the mixing time and can be used to provide a model for $\overline{uv}$, which is related to mean flow gradient transport.

Transport Producing Motions

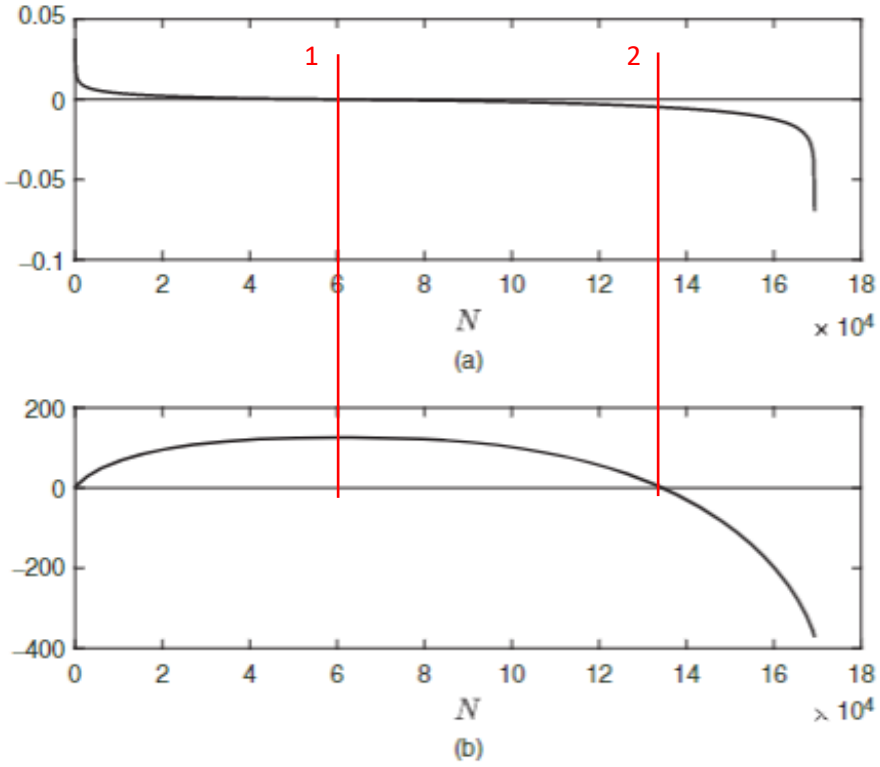

1: The cumulative sum starts to decrease because the additional contributions to $\overline{uv}$ have negative sign.

2: The cumulative sum becomes negative, showing that around 21% of the contributions are responsible for the negative sign of $\overline{uv}$.

Figure 6.6 Contributions to $\overline{uv}$ at $y^+ = 84.8$ from a data set consisting of 169,344 points in the lower channel half. (a) Individual contributions ranked from largest to smallest. (b) Cumulative sum of contributions in (a) showing zero crossing at $N_0 = 134{,}543$.

N paths that lead to $\overline{u_a v_a} < 0$, i.e., u_a and v_a opposite sign must take precedence than events same sign.

(a) Ranks from most + to most –

(b) partial sums $\sum u^i v^i$, a point is reached (N_0) where sign change from $+$ to $-$ $\therefore n > N_0$ responsible $\overline{uv} < 0$ since other contributions cancel out between $+$ and $-$. Fraction $(N - N_0)/N$ reveals useful information on how $\overline{uv}$ is created.

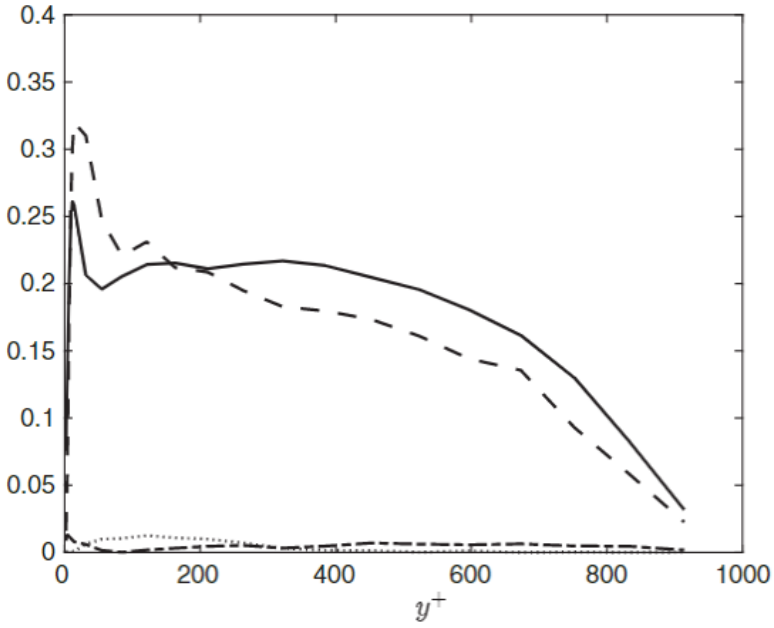

Plot for each term composing $\overline{u_a v_a}$ of the fraction of events (%) at each y^+ position whose contribution is not canceled by events with the opposite sign. Shows the contributions of $\overline{u_b v_a}$ and $\overline{v_a(U_a - U_b)}$ are linked to relatively rare events ≈1%

Figure 6.7 Fraction of points in the data ensembles that account for the local computed values of the terms in Eq. (6.24). —, $\overline{u_a v_a}$; – –, $\overline{(\overline{U}_b - \overline{U}_a)v_a}$; – · –, $\overline{(U_a - U_b)v_a}$; · · · , $\overline{u_b v_a}$.

$$\overline{u_a v_a} = \underbrace{\overline{u_b v_a}}_{1} + \underbrace{\overline{v_a(\langle U_b \rangle - \langle U_a \rangle)}}_{2} + \underbrace{\overline{v_a(U_a - U_b)}}_{3} \quad (5)$$

$\overline{u_a v_a}$ and terms 1,2 and 3 for $(N - N_0)/N$ fraction of events for time interval from $t - \tau_D$ to t. For large portion of the channel $\overline{u_a v_a}$ and Φ_D follow same trend. Fraction is generally 20% and rises to 30% at $y^+ = 30$. Towards the center of the channel, i.e., large $y+$, all the terms go to 0 due to $+$ and $-$ cancellation, as it would be expected in a symmetric flow.

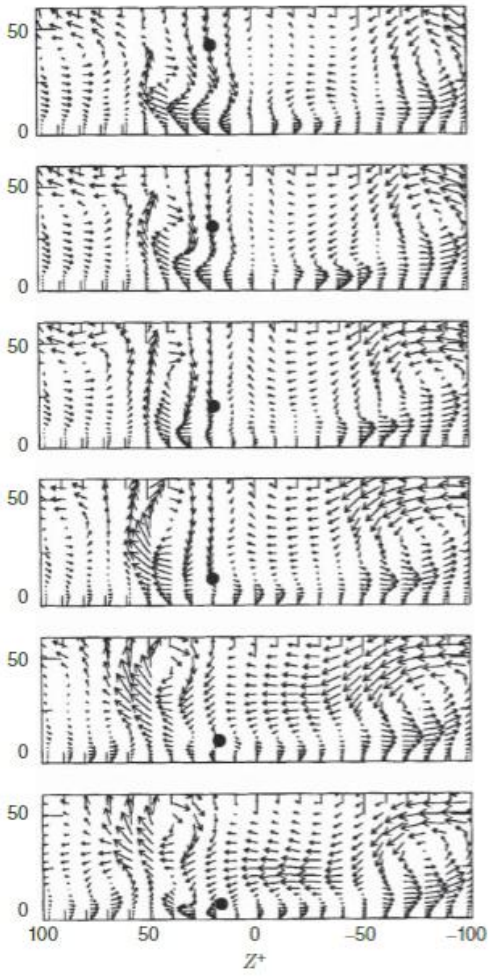

Figure 6.8 Fluid particle arriving at $y^+ = 7.3$ [7] due to a sweep event. Time increases moving from top to bottom image. Reprinted with the permission of Cambridge University Press.

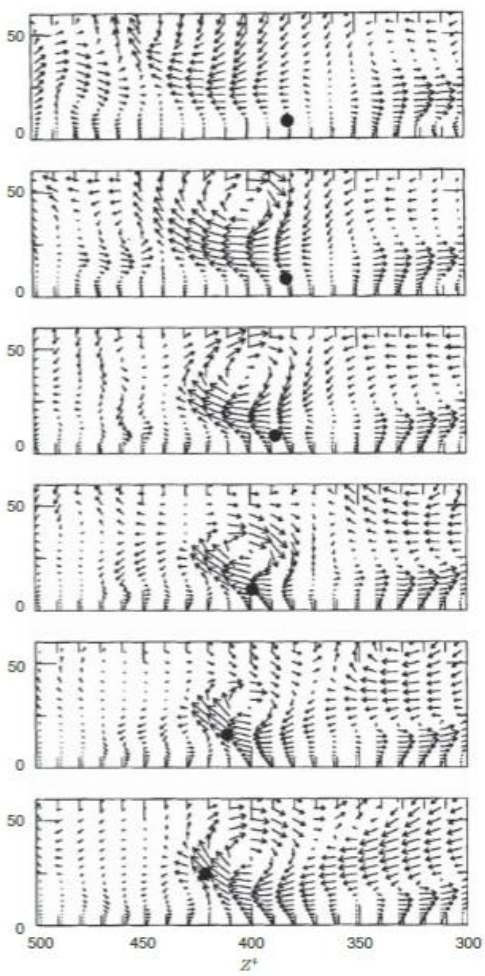

Figure 6.9 Fluid particle arriving at $y^+ = 24.6$ [7] due to an ejection event. Time increases moving from top to bottom image. Reprinted with the permission of Cambridge University Press.

Events that make significant contributions to $\overline{uv}$ → vortical eddies with streamwise orientation.

Sweep event: high speed flow towards wall, dominant contribution in buffer layer.

Ejection event: low speed flow ejected outward, occurs outside buffer layer.

Mixing time = time over which coherent vortices exert influence over motions of fluid particles.

Gradient Transport

If gradient transport is valid, it should be due to Φ_D under further hypothesis that change in local mean velocity along particle paths is linear such that a Taylor series can be used:

$$\underline{b} = \underline{a} - \underline{L}$$

$$\langle U_{\underline{b}} \rangle = \langle U_{\underline{a}-\underline{L}} \rangle$$

$$\overline{\langle U_{\underline{b}} \rangle} = \overline{U}_a - L_2 \frac{d\overline{U}}{dy} + \cdots$$

$$\underline{L} = \int_{t-\tau}^{t} \underline{U}\left(\underline{X}(s), s\right) ds$$

$$L_2(\tau) = \int_{t-\tau}^{t} v_b\left(\underline{X}(s), s\right) ds$$

$\bar{V} = 0$ as are $\frac{d\overline{U}}{dx} = \frac{d\overline{U}}{dz} = 0$

$$\Phi_D = \overline{\nu_a(\langle U_b \rangle - \overline{U}_a)} = \overline{\nu_a \left(\overline{U}_a - L_2 \frac{d\overline{U}}{dy} - \overline{U}_a + \cdots \right)} = -\overline{\nu_a L_2} \frac{d\overline{U}}{dy} + \cdots$$

which shows Φ_D equivalent gradient transport model; thus,

$$-\Phi_D \approx \overline{\nu_a L_2} \frac{\partial \overline{U}}{\partial y} \approx -\overline{uv}$$

Thus υ_T related $\overline{\nu_a L_2(\tau)}$; however, in this form depends on mixing time τ; since,

$$\overline{\nu_a L_2} = \int_{t-\tau}^{t} \nu_a \nu_b\left(\underline{X}(s), s\right) ds = \overline{\nu_a \nu_b}(\tau)$$

Which can be overcome by defining Lagrangian auto-correlation function:

$$f_{vv}(\tau) = \frac{\overline{\nu_a \nu_b}(\tau)}{\overline{\nu_a}^2}$$

similarly to what was done for the temporal autocorrelation function $R_E(\tau)$, the Lagrangian integral scale is defined by

$$\overline{\nu_a}^2 \mathcal{T}_{22} = \int_{-\infty}^{0} f_{vv}(\tau) d\tau$$

$\mathcal{T}_{22}$ like temporal Taylor macro scale Λ_t has units of t

And $f_{vv}(\tau) = 0$ for $|\tau|$ large, such that:

$$\int_{-\infty}^{0} \overline{\nu_a \nu_b}(\tau)\, d\tau = \overline{\nu_a}^2 \mathcal{T}_{22} = \nu_t \quad (6)$$

Shows gradient transport due to correlation between ν_a and ν_b = transverse velocity all fluid particles arriving a from $t - \tau$ based on Lagrangian integral scale $\mathcal{T}_{22}$.

If gradient transport were physically accurate then ν_t in Eq. (6) should approximate the eddy viscosity model

$$\nu_t = -\frac{\overline{uv}}{d\overline{U}/dy} = \text{physical } \nu_t \text{ vs. } \overline{\nu_a^2}\mathcal{T}_{22}$$

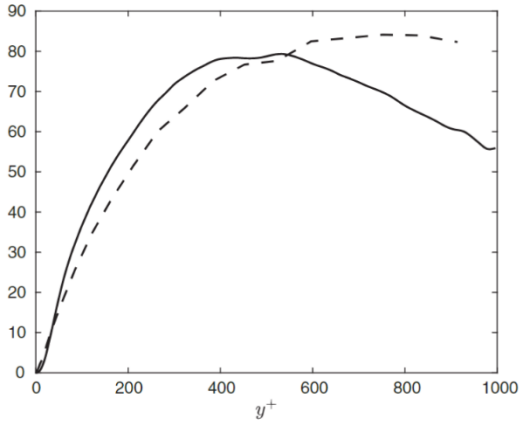

Figure 6.10 Eddy viscosity in channel flow: ––, $\mathcal{T}_{22}^+\overline{v^2}^+$; —, ν_t^+.

Same discrepancies for $y^+ > 500$ where physical ν_t = constant and modeled decreases; and near wall where physical < modeled. Note $\nu_t > 0$ over whole domain as per $d\overline{U}/dy$, except center channel where both equal 0; and vice versa for upper channel where $d\overline{U}/dy < 0$ and $\overline{uv} > 0$.

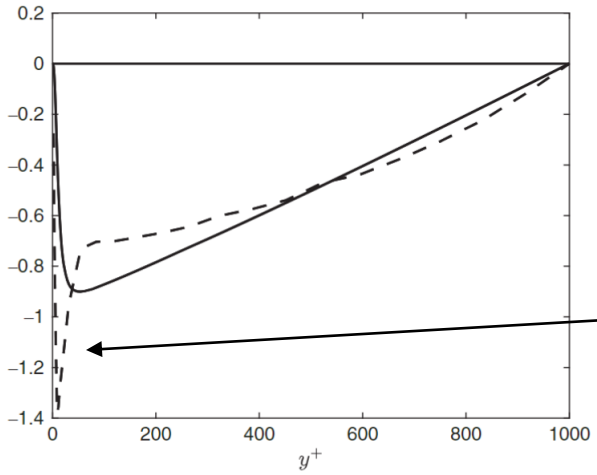

Near wall where gradient $\overline{U}$ largest and particles travel much greater distances than linear approximation

Figure 6.11 Inadequacy of gradient transport physics: —, $\overline{uv}^+$; ––, $-\mathcal{T}_{22}^+\overline{v^2}^+ d\overline{U}^+/dy^+$.

Obvious differences gradient transport vs actual $\overline{uv}$.

Large differences near wall, whereas smaller in outer part ∴ more suitable central part despite ν_t differences shown above.

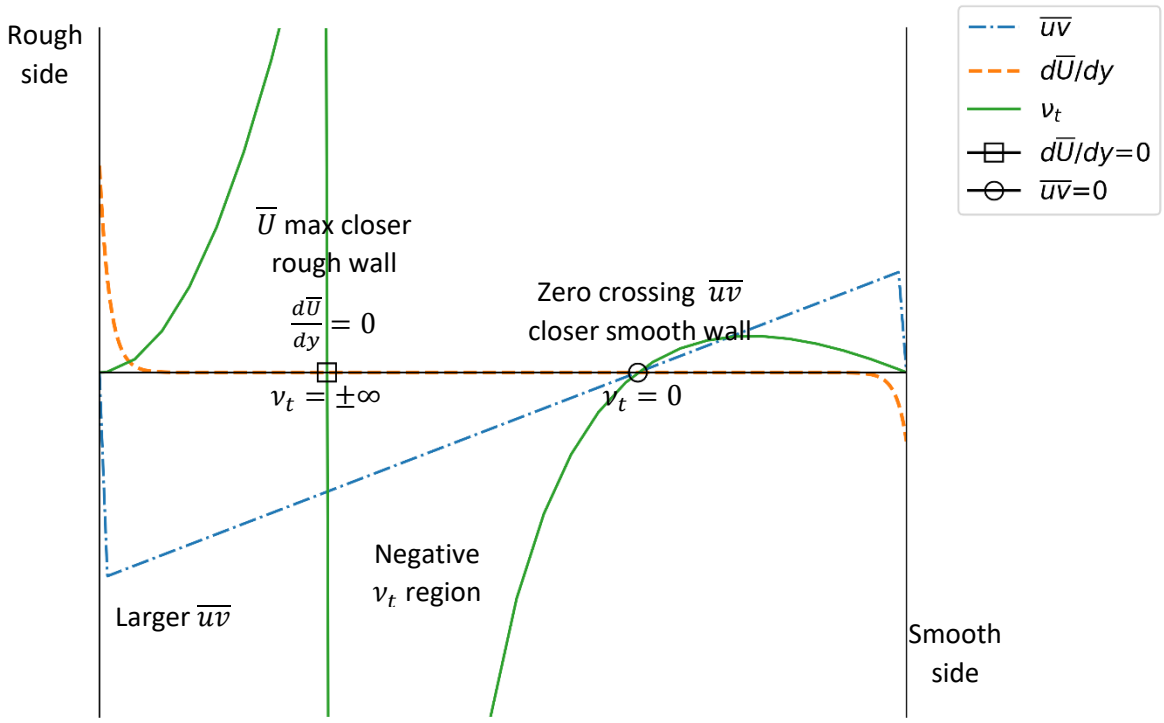

However, not satisfied for rough wall as ν_t shows unphysical behavior; and numerical methods unstable for $\nu_t < 0$.

$$\nu_t = -\frac{\overline{uv}}{d\overline{U}/dy}$$

Rough wall larger shear stress and $\overline{uv}$; therefore $\overline{U}$ max closer rough wall and $\frac{d\overline{U}}{dy} = 0$ closer rough wall; and since $\overline{uv}$ linear its zero crossing closer smooth wall, which creates zone in middle channel with $\nu_t < 0$. In fact, at $\frac{d\overline{U}}{dy} = 0$, $\nu_t = \infty$, i.e., unphysical.